17th World Conference on Earthquake Engineering, 17WCEE
Sendai, Japan - September 13th to 18th 2020

ENERGY WORKING MECHANISM AND OPTIMAL DESIGN FOR INERTER-BASED STRUCTURE

Z.P. Zhao[(1)], Q.J. Chen[(2)], R.F. Zhang [(3)], Y.Y. Jiang[(4)], C. Pan[(5)], X.S. Ren[(6)]

[(1)] *Doctorate candidate, Department of Disaster Mitigation for Structures, Tongji University, Shanghai, China, zhaozhipeng@tongji.edu.cn*
[(2)] *Professor, Department of Disaster Mitigation for Structures, Tongji University, Shanghai, China, chenqj@tongji.edu.cn*
[(3)] *Associate professor, Department of Disaster Mitigation for Structures, Tongji University, Shanghai, China, zhangruifu@tongji.edu.cn*
[(4)] *Master, Department of Disaster Mitigation for Structures, Tongji University, Shanghai, China, yyjiang17@fudan.edu.cn*
[(5)] *Associate professor, College of Civil Engineering, Yantai University, Yantai, China, panchao@ytu.edu.cn*
[(6)] *Professor, Department of Disaster Mitigation for Structures, Tongji University, Shanghai, China, rxs@mail.tongji.edu.cn*

Abstract

The inerter system has been proven to be an effective vibration control device, however, its energy-input-dissipation mechanism has not been clearly revealed. In this study, the closed-form energy equations are derived for the structure equipped with classic inerter systems, basically explaining their energy-related characteristic. The energy equations establish the theoretical relationship between the input energy, the dissipation energy and the key parameters of inerter system in an analytical form. Furthermore, the differences of the inerter systems comprising the grounded and ungrounded inerters are characterized through the comparative analysis in terms of the displacement control effect, energy dissipation efficiency, and reduction of the input energy. Correspondingly, a unified energy-dissipation-based design strategy is herein developed to optimize the displacement and energy-based responses of the structure as a dual-performance target control. Finally, numerical examples are presented to validate the derived energy equation and design strategy. The analysis results show that the energy equation yields the closed-form measurement to evaluate the input energy of the inerter-based structure and quantifies functionality of the inerter system for the energy dissipation. Especially, the energy equation explicitly reveals the basic fact that a grounded inerter can reduce the energy input into the entire inerter-based structure. Following the unified energy-dissipation-based design strategy, the target displacement demand can be satisfied quantitively by the optimized inerter systems, which also simultaneously optimizes the energy performance of the primary structure to relax its burden of energy dissipation.

Keywords: inerter; energy dissipation; analytical stochastic response; optimal design.

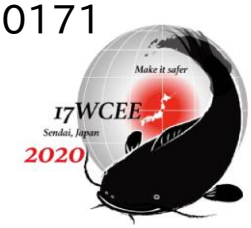

1. Introduction

The inerter-based control approach has attracted increased attention for vibration control in various engineering fields [1]. The inerter is a two-terminal inertial element that produces an inertance assuming mass unit while introducing negligible gravitational mass into the structure [2-5]. In an ideal linear scenario, the inertial force of this massless element is proportional to the relative acceleration between its two terminals. Known as the mass enhancement effect, the inertance can be thousands of times the gravitational mass of the inerter [6]. A series of "lightweight" tuned-type inerter systems [7-10] have been developed for effective vibration control at the cost of less tuned mass. In retrospect, ball-screw based inerter is employed into the traditional viscous damper to amplify the viscous damping force, which yields the mechanical realization of a basic inertia mass system that consists of a viscous damping element in parallel with an inerter. It is designated as a grounded inerter-dashpot system (IDS) in this study. Takewaki et al. [11] investigated the benefits of interstory inerters grounded directly to the floor to reduce the seismic response of buildings. Jiang et al. [12] proposed the analytical design formulae for the IDS installed in an isolation system for the multi-response control of a storage tank. Apart from the mentioned IDS, other typical inerter systems including the grounded inerter are tuned mass damper inerter [13] and tuned liquid inerter system [8].

In addition to the condition of grounded inerter, inerter systems comprising an ungrounded inerter have been proposed by inserting other mechanical elements between the inerter and the ground (floor) or the controlled structure, such as the tuned viscous mass damper (TVMD) [6] and tuned inerter damper [14]. For IDS and TVMD, Ikago et al. [6] figured out the important damping enhancement phenomenon that the dashpot deformation is amplified and larger than the deformation of the entire TVMD. Zhang et. al [15] derived closed-form damping enhancement equation to reveal the its basic working mechanism. Correspondingly, more vibrational energy is expected to be dissipated through the larger dashpot deformation, which is a benefit of implementing a tuned spring between the ground and IDS.

However, the theoretical basis for the energy-dissipation mechanism, and how to directly quantify the energy related to the dashpot deformation amplification effect remains unclear. The difference between the grounded and ungrounded inerters, has not been revealed in an analytical and explicit manner. In this study, a closed-form energy equation is derived to explain the theoretical basis and energy-input-dissipation characteristic of the IDS and TVMD, which are two typical inerter systems with grounded and ungrounded inerters, respectively. Furthermore, a unified energy-dissipation-based optimal design strategy is developed for the two inerter systems, as a dual-performance control to guarantee pre-specified displacement control demand with optimized energy dissipation cost imposed on the primary structure.

2. Energy equation

2.1 Mechanical models

Consider a viscously damped single-degree-of-freedom structure (Fig. 1), the primary structure is modeled by a mass m, a stiffness k, and a viscous damping coefficient c. Fig. 1 (a) shows the IDS that consists of a single grounded inerter with inertance m_{in} and a dashpot with damping coefficient c_d arranged in parallel without introducing any extra independent freedom. Through the insert of a tuned spring (k_d) between the ground and the IDS, the inerter system with a grounded inerter evolves into a classic inerter system, i.e. the TVMD, comprising an ungrounded inerter shown in Fig. 1 (b). From the perspective of mechanical layout and concerned displacement, the IDS is a special case of TVMD that takes the assumption of $k_d = \infty$.

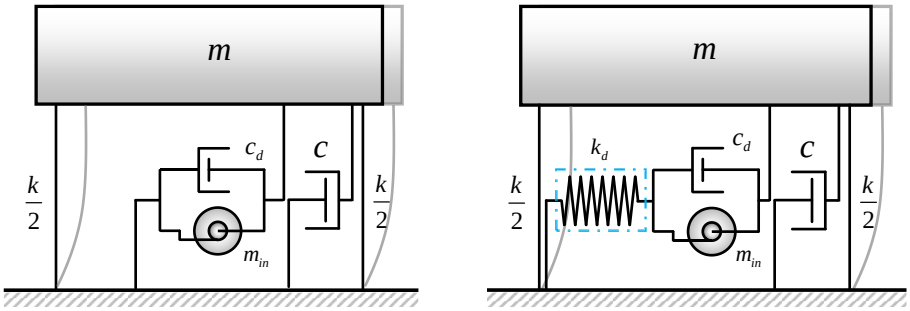

(a) Structure with IDS (b) Structure with TVMD

Fig. 1 – Mechanical models of considered inerter-based structures.

2.2. Motion governing equation and closed-form solutions

Subject to the base excitation $\ddot{u}_g$, the IDS structure, the governing equation is established according to dynamic equilibrium condition,

$$(1+\mu)\ddot{u}+2\omega_0(\zeta+\xi)\dot{u}+\omega_0^2 u=-\ddot{u}_g \tag{1}$$

where u is the displacement of the primary structure relative to the ground. Laplace transformation [16] is employed to obtain the Eq. (1) in an algebraic form.,

$$s^2U(1+\mu)+2s(\zeta+\xi)\omega_0 U+\omega_0^2 U=-\ddot{U}_g \tag{2}$$

where U and $\ddot{U}_g$ are the Laplace transformation forms of u and $\ddot{u}_g$, respectively, and $s=\mathrm{i}\omega$, where i is the imaginary unit and ω is the circular frequency of excitation. By solving Eq. (2) with respect to U, the structural response can be easily obtained. Supposing white noise with the amplitude of power spectra S_0 as the excitation, the mean-square of the displacement σ_U^2 and velocity of primary structure σ_{Vel}^2 can be derived in closed form [16],

$$\sigma_U^2=\frac{\pi S_0}{2(\zeta+\xi)\omega_0^3},\ \sigma_{Vel}^2=\frac{\pi S_0}{2(1+\mu)(\zeta+\xi)\omega_0} \tag{3}$$

By additionally considering the degree of dashpot deformation u_d, the similar derivation for the TVMD structure is conducted [16], where relevant velocity response of primary structure σ_{Vel}^2 and dashpot $\sigma_{Vel,d}^2$ are given in detail:

$$\begin{cases}\sigma_{Vel}^2=\dfrac{\pi S_0}{2\omega_0}\dfrac{4\zeta^2\kappa\mu\xi+\zeta\left(\kappa^2\mu^2+4\mu\xi^2+4\kappa(1+\mu)\xi^2\right)+\xi\left(\mu^2+\kappa^2\left(1-\mu+\mu^2\right)+4\xi^2+2\kappa\left(-\mu+\mu^2+2\xi^2\right)\right)}{4\zeta^3\kappa\mu\xi+\kappa^2\xi^2+\zeta^2\left(\kappa^2\mu^2+4\mu\xi^2+4\kappa(1+\mu)\xi^2\right)+\zeta\xi\left(\mu^2+\kappa^2\left(1+\mu^2\right)+4\xi^2+2\kappa\left(-\mu+\mu^2+2\xi^2\right)\right)}\\ \sigma_{Vel,d}^2=\dfrac{\pi S_0}{2\omega_0}\dfrac{\kappa^2(\zeta\mu+\xi)}{4\zeta^3\kappa\mu\xi+\kappa^2\xi^2+\zeta^2\left(\kappa^2\mu^2+4\mu\xi^2+4\kappa(1+\mu)\xi^2\right)+\zeta\xi\left(\mu^2+\kappa^2\left(1+\mu^2\right)+4\xi^2+2\kappa\left(-\mu+\mu^2+2\xi^2\right)\right)}\end{cases} \tag{4}$$

2.3. Energy-balance analysis

Compared to the displacement- or acceleration-based performance indices, the energy-balance analysis yields a more stable result, and is thus more robust against various types of input ground motion. To characterize the dynamic behavior of the IDS structure, an energy-balance analysis model is established by pre-multiplying Eq. (1) by $\dot{u}$, and then integrating over the time domain. The input energy can finally be distributed into the contributions,

$$E_{k,s}(t)+E_{d,s}(t)+E_{e,s}(t)+E_{k,IDS}(t)+E_{d,IDS}(t)=E_{input}(t) \tag{5}$$

where $E_{k,s}(t)=\int_0^t \dot{u}\ddot{u}\mathrm{d}t$, $E_{d,s}(t)=\int_0^t \dot{u}\cdot 2\zeta\omega_0\dot{u}\mathrm{d}t$, $E_{e,s}(t)=\int_0^t \dot{u}\omega_0^2 u\mathrm{d}t$, and $E_{input}(t)=\int_0^t \dot{u}\ddot{u}_g\mathrm{d}t$ are the integral of the kinetic energy, viscous damping energy, elastic strain energy of the primary structure, and input energy, respectively; and $E_{k,IDS}(t)=\int_0^t \dot{u}\mu\ddot{u}\mathrm{d}t$ and $E_{d,IDS}(t)=\int_0^t \dot{u}\cdot 2\xi\omega_0\dot{u}\mathrm{d}t$ are the integral of the kinetic energy and viscous damping energy of IDS, respectively. The energy balance for unit time can be established as

$$e_{k,s}+e_{d,s}+e_{e,s}+e_{k,IDS}+e_{d,IDS}=e_{input} \tag{6}$$

where the generic notation e_x represents the rate of energy (i.e. the power) E_x at the time instance t [17]. Consider energy-balance analysis dealing with stochastic excitation $\ddot{u}_g$; the input power and dissipation power can be evaluated stochastically by applying the expectation operator $\mathrm{E}[\cdot]$ to the terms of the integral in Eq. (6). Consistently with the conservation of mechanical energy, $\mathrm{E}[e_{d,s}]$, $\mathrm{E}[e_{d,IDS}]$ are equal to zero, $\mathrm{E}[e_{d,s}]=2\zeta\omega_0\mathrm{E}[\dot{u}\dot{u}]=2\zeta\omega_0\sigma_{Vel}^2$ and $\mathrm{E}[e_{d,IDS}]=2\xi\omega_0\mathrm{E}[\dot{u}\dot{u}]=2\zeta\omega_0\sigma_{vel}^2$. Substituting the closed-form expression σ_{Vel}^2 into above expressions, the input power of the entire IDS structure in the stationary condition is finally obtained as

$$\mathrm{E}[e_{input}]=2\zeta\omega_0\sigma_{Vel}^2+2\xi\omega_0\sigma_{Vel}^2=2(\zeta+\xi)\omega_0\cdot\frac{\pi S_0}{2(1+\mu)(\zeta+\xi)\omega_0}=\frac{\pi S_0}{(1+\mu)} \tag{7}$$

It should be noted that, under the stationary condition, the input power is equal to the sum of the dissipation powers produced by the primary structure and inerter system. With regard to an uncontrolled structure, the corresponding input power is easily obtained as a special case of Eq. (7) by designating $\mu=0$, which can be expressed as $\mathrm{E}[e_{input,0}]=2\zeta\omega_0\sigma_{Vel,0}^2=\pi S_0$, where the subscript '0' refers to the condition of an uncontrolled SDOF structure. The dimensionless velocity response ratios of the primary structure α and inerter system β are defined to evaluate the dissipation power produced by the viscous damping of the primary structure and the inerter system, whereas the normalized input energy ratio η is given as

$$\alpha=\frac{\sigma_{Vel}}{\sigma_{Vel,0}},\ \beta=\frac{\sigma_{Vel,d}}{\sigma_{Vel,0}},\ \eta=\frac{\mathrm{E}[e_{input}]}{\mathrm{E}[e_{input,0}]} \tag{8}$$

Dividing both sides of Eq. (7) by $2\zeta\omega_0\sigma_{Vel,0}^2$, it is simplified as by referring to the defined dimensionless ratios

$$\frac{2\zeta\omega_0\sigma_{Vel}^2+2\xi\omega_0\sigma_{Vel}^2}{2\zeta\omega_0\sigma_{Vel,0}^2}=\alpha^2+\frac{\xi}{\zeta}\beta^2,\ \eta=\frac{\mathrm{E}[e_{input}]}{2\zeta\omega_0\sigma_{Vel,0}^2}=\frac{\mathrm{E}[e_{input}]}{\mathrm{E}[e_{input,0}]}=\frac{1}{1+\mu} \tag{9}$$

For the IDS structure, the α is equal to the β because of the same displacements of the primary structure and the dashpot in the IDS. On the basis of Eq. (9), the energy equation finally reads as

$$\alpha^2+\frac{\xi}{\zeta}\beta^2=\eta,\ \left(\eta=\frac{1}{1+\mu}\right) \tag{10}$$

where $\eta=\frac{1}{1+\mu}$ is the input energy ratio and reflects the significant reduction of input power owing to the implementation of the grounded inerter. α^2 and $\beta^2\xi/\zeta$ represent the dissipation powers of the primary structure and the IDS, respectively.

Repeating the same energy-balance analysis for the TVMD structure, it can be obtained as

$$\mathrm{E}\left[e_{input}\right]=2\zeta\omega_0\sigma_{Vel}^2+2\xi\omega_0\sigma_{Vel,d}^2=\pi S_0\frac{D-\left(\kappa^2\xi^2+\zeta\xi\mu\right)}{D}+\pi S_0\frac{\left(\kappa^2\xi^2+\zeta\xi\mu\right)}{D}=\pi S_0 \tag{11}$$

where,

$$D=4\zeta^3\kappa\mu\xi+\kappa^2\xi^2+\zeta^2\left(\kappa^2\mu^2+4\mu\xi^2+4\kappa\left(1+\mu\right)\xi^2\right)+\zeta\xi\left(\mu^2+\kappa^2\left(1+\mu^2\right)+4\xi^2+2\kappa\left(-\mu+\mu^2+2\xi^2\right)\right) \tag{12}$$

Dividing both sides of Eq. (11) by $2\zeta\omega_0\sigma_{Vel,0}^2$, the energy equation for TVMD reads as

$$\alpha^2+\frac{\xi}{\zeta}\beta^2=\eta,\ (\eta=1) \tag{13}$$

Referring to the energy balance revealed by the energy Eq. (10) and Eq. (13), $\eta=\frac{1}{1+\mu}$ in Eq. (10) is lower than $\eta=1$ in Eq. (13); therefore, in an IDS structure (Fig. 1 (a)), implementation of an inerter between the controlled structure and excitation source (ground) can significantly reduce the input power compared with the cases of the TVMD structure (Fig. 1 (b)).

3. Unified energy-dissipation-based design

3.1 Design equations

Following the derived energy equation and energy working mechanism, a unified optimal design framework is proposed for the inerter system with grounded or ungrounded inerter, i.e., the IDS and the TVMD respectively. Taking the displacement and energy performance control into consideration, it is preferentially suggested for the primary structure to achieve a dual-control, which are represented by γ and α^2, respectively. Once the displacement response factor γ is selected as a measurement of the vibration control effect of an inerter system (for instance the target demand of displacement γ_t), the energy-based factors for the primary structure (α^2) is the key supplementary indicator to be minimized for releasing the control cost and the energy dissipation burden imposed on the primary structure.

$$\gamma=\frac{\sigma_U}{\sigma_{U,0}} \tag{14}$$

Correspondingly, the unified optimal design problem of the IDS and TVMD is expressed in a mathematical form,

$$\begin{cases}\text{Minimize}\quad \text{energy cost } \alpha^2\\ \text{subject to}\quad \begin{cases}\gamma=\gamma_t\\ v\in V\end{cases}\end{cases} \tag{15}$$

where v is the variable vector of the IDS parameters ($v=\{\mu,\ \xi\}$) or the TVMD parameters ($v=\{\mu,\ \xi,\ \kappa\}$); V is the considered feasible domain of the v. Integrating the difference of the energy working basis between the IDS and TVMD, the unified design problem in Eq. (15) can yield targeted design equations for the two systems as follows.

The design of IDS includes the determination of two key parameters, namely μ and ξ. According to the closed-form expressions of σ_U^2 (related to γ) in an IDS structure, the displacement response control effect γ_t is totally dependent on the damping ratio ξ for a structure with given ζ. Correspondingly, the first-line step is to determine the damping ratio ξ to quantify the specific level of γ. Then, referring to the

σ_{Vel}^2 (related to α^2), the α^2 is inversely proportional to the implemented inertance-mass ratio μ, of which the derivative with respect to μ is

$$\frac{\partial \alpha^2}{\partial \mu} = -\frac{\zeta}{(1+\mu)^2(\zeta+\xi)} < 0 \tag{16}$$

The minimization of the α^2 in the unified design Eq. (15) lies in the upper boundary of μ, which is consistent with the minimization of input energy ratio η in Eq. (10). In this situation, the desired target reduction of the input energy η_t is integrated into the IDS design to determine the value of the upper boundary of μ, potentially reducing the input energy and control the force of the dashpot. To sum up, the design equation of IDS is expressed as,

$$\begin{cases} \xi = \zeta\left(\dfrac{1}{\gamma_t^2} - 1\right) \\ \mu = \dfrac{1}{\eta_t} - 1 \end{cases} \tag{17}$$

For TVMD, there exist three key parameters to be designed, the μ, ξ, and κ. As revealed in the energy Eq. (13), the input power into the TVMD structure is unit, which is different from the case of a structure with a grounded inerter. Referring to the parametric analysis results of γ and α^2 in Fig. 2, for a TVMD structure with a temporarily given tuned spring κ, the variation patterns of γ and α^2 resemble a valley topology, for which the basin (marked by the yellow and white triangles for γ and α^2, respectively) denotes to the lowest value. The yellow and white triangles locate near each other, implying that the parameter set marked by the triangle is an efficient solution to determine μ and ξ for the simultaneous control of displacement response and energy dissipation.

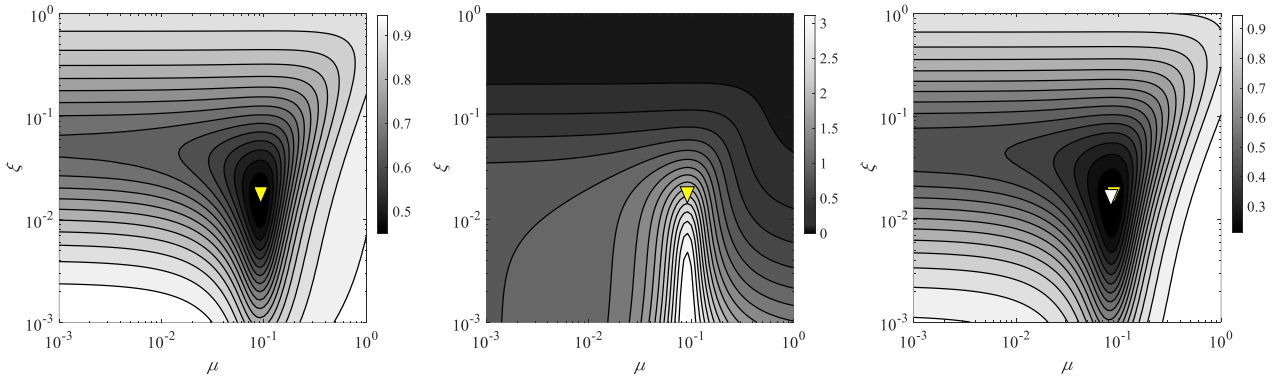

(a) (b) (c)

Fig. 2 – Contour curves of γ, λ, and α^2 of TVMD structure for $\zeta = 0.02$, $\mu \in [0.001, 1.0]$, and $\xi \in [0.001, 1.0]$, where minimum γ and α^2 are marked by the yellow and white triangles, respectively. (a) Displacement response ratio γ, (b) dashpot deformation amplification ratio λ, and (c) energy dissipated by structure α^2.

In this section, the pursuit of minimum α^2 (the white triangle) can be interpreted as the partial derivative of α^2 with respect to μ, with ξ set zero. Hence, the dual-performance control problem of TVMD is finally expressed in mathematical form as

$$\begin{cases} \text{Minimize} \quad \alpha^2(\mu,\xi,\kappa) \\ \text{subject to} \quad \gamma(\mu,\xi,\kappa)=\gamma_t \end{cases} \rightarrow \begin{cases} \text{Solve} \quad \gamma(\mu,\xi,\kappa)=\gamma_t \\ \text{subject to} \begin{cases} \dfrac{\partial \alpha^2}{\partial \mu}=0 \\ \dfrac{\partial \alpha^2}{\partial \xi}=0 \end{cases} \end{cases}. \tag{18}$$

Substituting the closed-form expression of α^2 of Eq. (4) into Eq. (18), the values of μ and ξ can be determined theoretically, although the detailed expression is complicated. Considering that the inherent damping ratio ζ of the superstructure is always small, the analytical expressions of μ and ξ can be simplified as functions of κ by assuming that $\zeta=0$:

$$\mu=\frac{\kappa(2+\kappa)}{2(1+\kappa)^2},\ \xi=\frac{1}{4}\sqrt{\frac{\kappa^3(4+3\kappa)}{(1+\kappa)^3}}. \tag{19}$$

which can be further used in the conceptional design.

3.2 Design cases

Utilizing the proposed energy-dissipation-based optimal design strategy, an illustrative example of typical IDS and TVMD structures are designed and analyzed. At the same time, the differences between IDS and TVMD in terms of displacement response control and energy dissipation are characterized by the comparison. After the initial dynamic analysis of the original uncontrolled structure, the dynamic performance is improved by IDS or TVMD, where γ_t is assumed as 0.30. Considering the determined value of γ_t, the IDS and TVMD are obtained analytically from Eqs. (17) and (18), whose results are summarized in Table 1.

Table 1. Designed inerter system parameters and structural response results.

Case IDS	Pre-specified		Optimal parameters			Structural responses
	γ_t	η_t	ξ	μ	κ	$\alpha^2(=\beta^2)$
Case-A	0.30	0.50	0.202	1.000	-	0.045
Case-B	0.30	-	0.115	0.278	0.580	0.094

To further characterize the dynamic performances of IDS and TVMD structures under white noise and more realistic excitation, time history analyses were conducted for white noise and N–S records of the El Centro 1940 earthquake. The intensity measure of the excitation (for instance, the peak ground acceleration) does not affect the results in terms of vibration control ratios, under the assumption of the postulated linear behavior of the controlled system. Considering Case-A and -B, the structural displacement u is shown in Fig. 3, of which the corresponding values of the displacement response ratio γ are also calculated and are depicted in the figures.

For both the white noise and actual excitation, the structural displacement is reduced effectively by IDS and TVMD, whose γ matches the pre-specified values shown in the title of the figure. This reflects the fact that the proposed energy-dissipation-based optimal strategy under the assumption of white-noise excitation can also produce a satisfactory performance for a structure subject to real excitation. Fig. 4 plots the hysteretic curves of the inherent damping element of primary structures with the same ζ, in which the maximum damping deformation and maximum damping force of the IDS structure are lower than those of the TVMD structure. For Case-A and B, IDS and TVMD are designed under the same γ_t to provide the primary structure with the same mean-square displacement responses. Benefiting from the grounded inerter, the total energy input into the IDS structure is much lower than that of the TVMD structure, as shown in Fig. 5, which relaxes the energy-dissipation burden of the primary structure and inerter-based system.

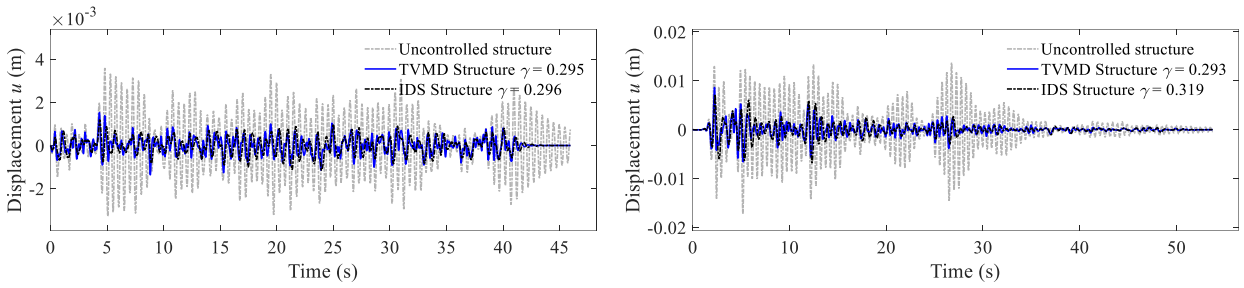

(a) (b)

Fig. 3 – Displacement responses of an uncontrolled structure and structures with an IDS and a TVMD for Case-A and B ($\gamma = 0.30$). (a) White noise and (b) El Centro earthquake.

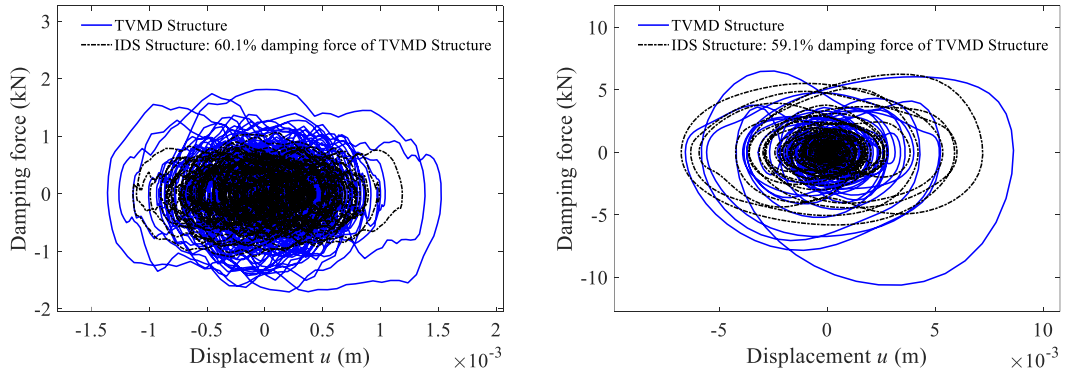

(a) (b)

Fig. 4 – Hysteretic curves of structural inherent damping elements for Case-A and B ($\gamma = 0.30$). (a) White noise and (b) El Centro earthquake.

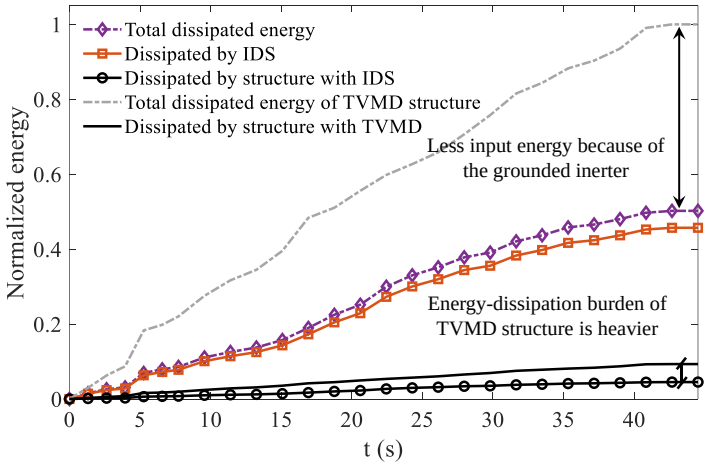

Fig. 5 – Normalized energy curves of structures with an IDS and a TVMD in Case-A and B ($\gamma = 0.30$) under excitation of the white noise. (a) Structure with TVMD and (b) structure with IDS.

4. Conclusions

This study derives a closed-form energy equation and proposes a unified energy-dissipation-based optimal design strategy to achieve dual-performance control. The main conclusions of this study can be summarized as follows:

(1) Energy equations explicitly establish the theoretical relationship between the input power, dissipation power, and parameters of inerter system, which can explain the energy-input-dissipation mechanism of the inerter systems in a direct manner.

(2) Inerter systems comprising a grounded inerter have the dual benefits of reducing the input power and energy into the entire inerter-based controlled structure and dissipating the vibrational energy at the same time.

(3) Employing the energy equation, the unified energy-dissipation-based optimal design strategy effectively minimizes the burden of dissipated energy contributed by the inherent damping of the primary structure, simultaneously providing a satisfactory displacement performance.

5. Acknowledgements

This study was supported by the National Natural Science Foundation of China (grant no. 51978525 and 51778489) and the Natural Science Foundation of Shandong Province, China (grant no. ZR2018BEE033).

6. Copyrights

7. References

[1] Chen MZQ, Hu Y, Li C, Chen G (2015), Performance benefits of using inerter in semiactive suspensions, IEEE Transactions on Control Systems Technology, **23**, 1571-1577.

[2] Chen QJ, Zhao ZP, Zhang RF, Pan C (2018), Impact of soil–structure interaction on structures with inerter system, Journal of Sound & Vibration, **433**, 1-15.

[3] Zhao ZP, Zhang RF, Jiang YY, De Domenico D, Pan C (2019), Displacement-dependent damping inerter system for seismic response control, Applied Sciences, **10** (1), 257.

[4] Makris N, Moghimi G (2019), Displacements and forces in structures with inerters when subjected to earthquakes, Journal of Structural Engineering, **145** (2), 04018260.

[5] John EDA, Wagg DJ (2019), Design and testing of a frictionless mechanical inerter device using living-hinges, Journal of the Franklin Institute, **356**, 7650-7668.

[6] Ikago K, Saito K, Inoue N (2012), Seismic control of single-degree-of-freedom structure using tuned viscous mass damper, Earthquake Engineering and Structural Dynamics, **41**, 453-474.

[7] Zhao ZP, Zhang RF, Lu Z (2019), A particle inerter system for structural seismic response mitigation, Journal of the Franklin Institute, **356**, 7669-7688.

[8] Zhao ZP, Zhang RF, Jiang YY, Pan C (2019), A tuned liquid inerter system for vibration control, International Journal of Mechanical Sciences, **164**, 105171.

[9] Zhang RF, Zhao ZP, Dai KS (2019), Seismic response mitigation of a wind turbine tower using a tuned parallel inerter mass system, Engineering Structures, 180, 29-39.

[10] Chen QJ, Zhao ZP, Xia YY, Pan C, Luo H, Zhang RF (2019), Comfort-based floor design employing tuned inerter mass system, Journal of Sound and Vibration, **458**, 143-157.

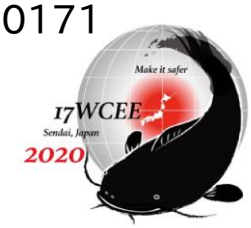

[11] Takewaki I, Murakami S, Yoshitomi S, Tsuji M (2012), Fundamental mechanism of earthquake response reduction in building structures with inertial dampers, Structural Control and Health Monitoring, **19**, 590-608.

[12] Jiang YY, Zhao ZP, Zhang RF, De Domenico D, Pan C (2020), Optimal design based on analytical solution for storage tank with inerter isolation system, Soil Dynamics and Earthquake Engineering, **129**, 105924.

[13] Marian L, Giaralis A (2014), Optimal design of a novel tuned mass-damper–inerter (TMDI) passive vibration control configuration for stochastically support-excited structural systems, Probabilistic Engineering Mechanics, **38**, 156-164.

[14] Lazar IF, Neild SA, Wagg DJ (2016), Vibration suppression of cables using tuned inerter dampers, Engineering Structures, **122**, 62-71.

[15] Zhang RF, Zhao ZP, Pan C, Ikago K, Xue ST (2020), Damping enhancement principle of inerter system, Structural Control and Health Monitoring, e2523.

[16] Crandall SH, Mark WD (2014), Random Vibration in Mechanical System, Academic Press.

[17] Reggio A, Angelis MD (2015), Optimal energy-based seismic design of non-conventional Tuned Mass Damper (TMD) implemented via inter-story isolation, Earthquake Engineering & Structural Dynamics, **44**, 1623-1642.

